Earth and Planetary Science Letters 510 (2019) 1–11

Contents lists available at ScienceDirect

Earth and Planetary Science Letters

www.elsevier.com/locate/epsl

Dynamic storage of glacial CO_2 in the Atlantic Ocean revealed by boron $[CO_3^{2-}]$ and pH records

T.B. Chalk [a,b,*], G.L. Foster [a], P.A. Wilson [a]

[a] School of Ocean and Earth Science, University of Southampton, Waterfront Campus, National Oceanography Centre Southampton, Southampton, SO14 3ZH, UK
[b] Department of Physical Oceanography, Woods Hole Oceanographic Institution, Woods Hole, MA, 02543, USA

ARTICLE INFO

Article history:
Received 4 March 2018
Received in revised form 6 December 2018
Accepted 21 December 2018
Available online xxxx
Editor: J. Adkins

Keywords:
boron
geochemistry
palaeoceanography
carbonate system
glacial
Atlantic

ABSTRACT

The origin and carbon content of the deep water mass that fills the North Atlantic Basin, either Antarctic Bottom Water (AABW) or North Atlantic Deep Water (NADW) is suggested to influence the partitioning of CO_2 between the ocean and atmosphere on glacial–interglacial timescales. Fluctuations in the strength of Atlantic meridional overturning circulation (AMOC) have also been shown to play a key role in global and regional climate change on timescales from annual to millennial. The North Atlantic is an important and well-studied ocean basin but many proxy records tracing ocean circulation in this region over the last glacial cycle are challenging to interpret. Here we present new B/Ca-$[CO_3^{2-}]$ and boron isotope-pH data from sites spanning the North Atlantic Ocean from 2200 to 3900 m and covering the last 130 kyr from both sides of the Mid-Atlantic Ridge. These data allow us to explore the potential of the boron-based proxies as tracers of ocean water masses to ultimately identify the changing nature of Atlantic circulation over the last 130 kyr. This possibility arises because the B/Ca and boron isotope proxies are directly and quantitatively linked to the ocean carbonate system acting as semi-conservative tracers in the modern ocean. Yet the utility of this approach has yet to be demonstrated on glacial–interglacial timescales when various processes may alter the state of the deep ocean carbonate system. We demonstrate that the deep (~3400 m) North Atlantic Ocean exhibits considerable variability in terms of its carbonate chemistry through the entirety of the last glacial cycle. Our new data confirm that the last interglacial marine isotope stage (MIS) 5e has a similar deep-water geometry to the Holocene, in terms of the carbonate system. In combination with benthic foraminiferal $\delta^{13}C$ and a consideration of the $[CO_3^{2-}]$ of contemporaneous southern sourced water, we infer that AABW influences the eastern abyssal North Atlantic throughout the whole of the last glacial (MIS2 through 4) whereas, only in the coldest stages (MIS2 and MIS4) of the last glacial cycle was AABW an important contributor to our deep sites in both North Atlantic basins. Taken together, our carbonate system depth profiles reveal a pattern of changing stratification within the North Atlantic that bears strong similarities to the atmospheric CO_2 record, evidencing the important role played by ocean water mass geometry and the deep ocean carbonate system in driving changes in atmospheric CO_2 on these timescales.

1. Introduction

Over the last 3 million years, Earth's climate has oscillated between interglacial conditions, much like the pre-industrial, and relatively cold glacials, when global sea-levels were ~130 m lower and global temperatures ~4 °C cooler than the pre-industrial (Crowley, 2000; Grant et al., 2014). For at least the last 800 kyr the glacial–interglacial climate cycles varied together with, and were amplified by, changes in atmospheric CO_2 concentrations (low/high during glacials/interglacials; Bereiter et al., 2015; Broecker and Denton, 1989). The most recent glacial termination (Termination I; T1) occurred <20 kyrs ago and, although a wealth of proxy records are available for this important interval, the forcing and amplifying mechanisms responsible for the repeating glaciation and deglaciation cycles in the Pleistocene remain far from fully understood (e.g. Kohfeld and Ridgwell, 2013). However, because the oceans are the only large exogenic carbon storage reservoir that can respond on such rapid timescales, it is highly likely that changes in ocean carbon storage play a major role in (sub)millennial-scale changes

* Corresponding author at: School of Ocean and Earth Science, University of Southampton, Waterfront Campus, National Oceanography Centre Southampton, Southampton, SO14 3ZH, UK.
E-mail address: t.chalk@noc.soton.ac.uk (T.B. Chalk).

https://doi.org/10.1016/j.epsl.2018.12.022

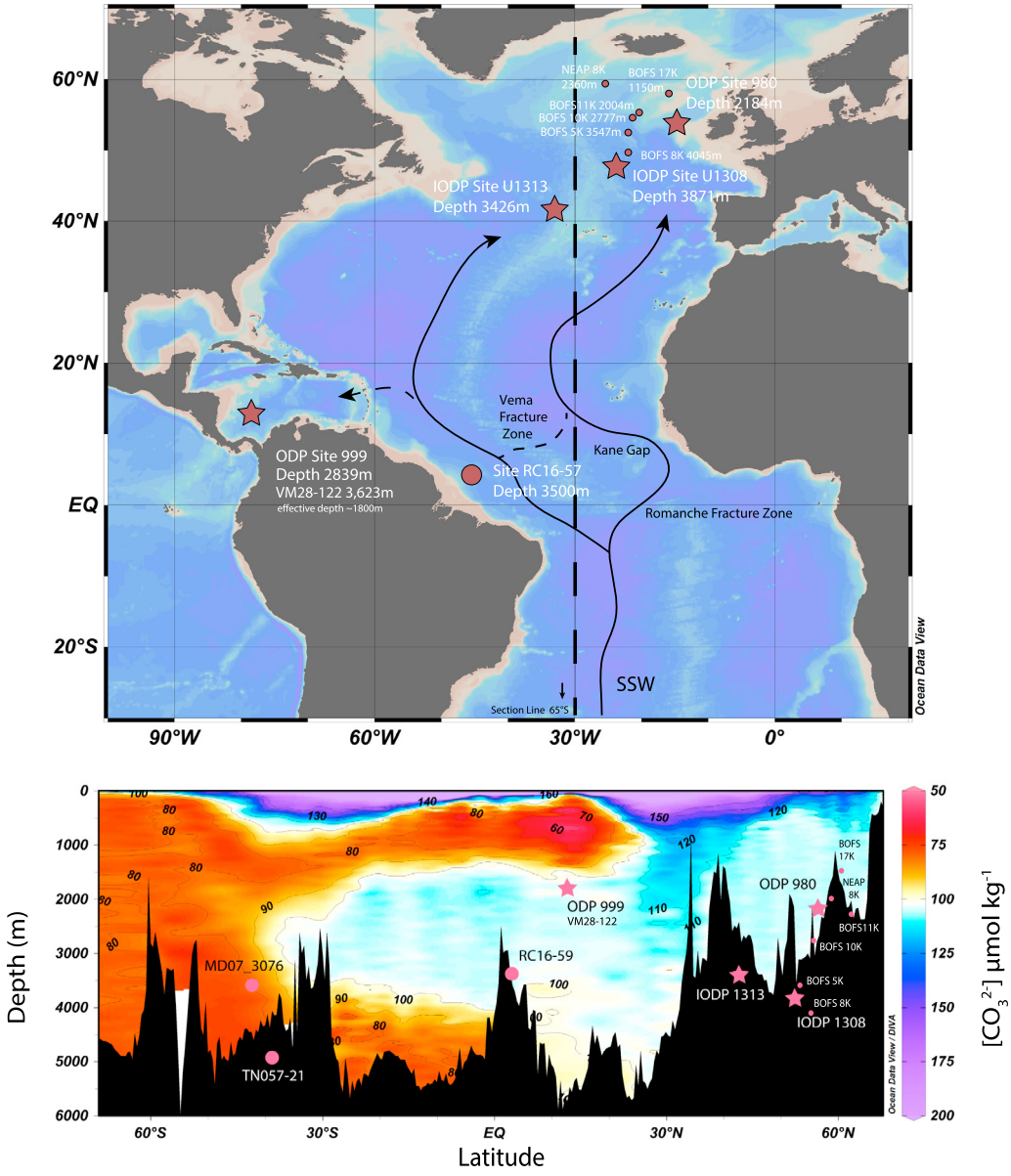

Fig. 1. Site map and section. a: Locations of the cores used in this study, ODP Sites 980 and 999, and IODP Sites U1308 and U1313 present a depth, latitude and longitude transect of the North Atlantic. Flow of modern deep water is indicated by the arrows – after Raymo et al. (2004) modified from Yu et al. (2008), dashed lines indicate Intermediate water pathways over the Caribbean sill (depth ∼1.8 km), map was created using Ocean Data View (Schlitzer, 2009). Abbreviations are: NGS, Norwegian–Greenland Sea; DSOW, Denmark Strait Overflow Water; ISOW, Iceland Sea Overflow Water; WTRO, Wyville Thomas Ridge Overflow; LSW, Labrador Seawater (together make up NSW); and SSW, Southern Sourced (deep) Water. Also shown are the other published cores sites used in this study. b: A section plot of the Atlantic using GLODAPv2 data (Key et al., 2015) for $[CO_3^{2-}]$, also showing the sites used in this study, the water mass divides between NADW and SSW are clearly visible between high and low $[CO_3^{2-}]$, respectively. (For interpretation of the colours in the figure(s), the reader is referred to the web version of this article.)

in atmospheric CO_2 and hence climate (Ahn and Brook, 2008; Martinez-Boti et al., 2015). Thus, it is important to determine where in the deep ocean atmospheric CO_2 is sequestered during glacial intervals in order to glean further insight to what mechanism(s) is (are) responsible for changing the relative partitioning of CO_2 between the atmosphere and the ocean. Among the many suggested mechanisms for glacial ocean CO_2 storage (e.g. Archer et al., 2000; Brovkin et al., 2012; Hain et al., 2010; Sigman et al., 2010) the expansion of Dissolved Inorganic Carbon (DIC)-rich $[CO_3^{2-}]$-poor Antarctic Bottom Water (AABW) into the North Atlantic basin is suggested to account for up to ∼50% of the CO_2 decline observed associated with the transition from the last interglacial to the last glacial maximum (Brovkin et al., 2012; Hain et al., 2010; Skinner, 2009) while an increase in the C-storage in the deep ocean particularly through changes in nutrient utilisation and stratification in the Southern Ocean is suggested to be the other major process enhancing whole ocean storage (Burke and Robinson, 2012; Rae et al., 2018; Toggweiler, 1999).

Changes in the patterns of North Atlantic circulation (see Fig. 1) are supported by many proxy records (e.g. carbon and oxygen isotopes, and Cd/Ca and Mg/Ca ratios of benthic foraminiferal calcite, e.g. Curry and Oppo (2005); Gebbie (2014), as well as neodymium isotopes (ε_{Nd}) (e.g. Böhm et al., 2015; Howe et al., 2016) with the standing hypothesis being that expansion and contraction of AABW accounts for a substantial component of the ocean–atmosphere glacial–interglacial CO_2 variability (Sigman et al., 2010; Skinner, 2009), because more of this carbon-rich water locked away in the deep ocean isolates CO_2 from the atmosphere. Determining the magnitude of this AABW expansion/contraction is key, because different proxy and modelling solutions demand dif-

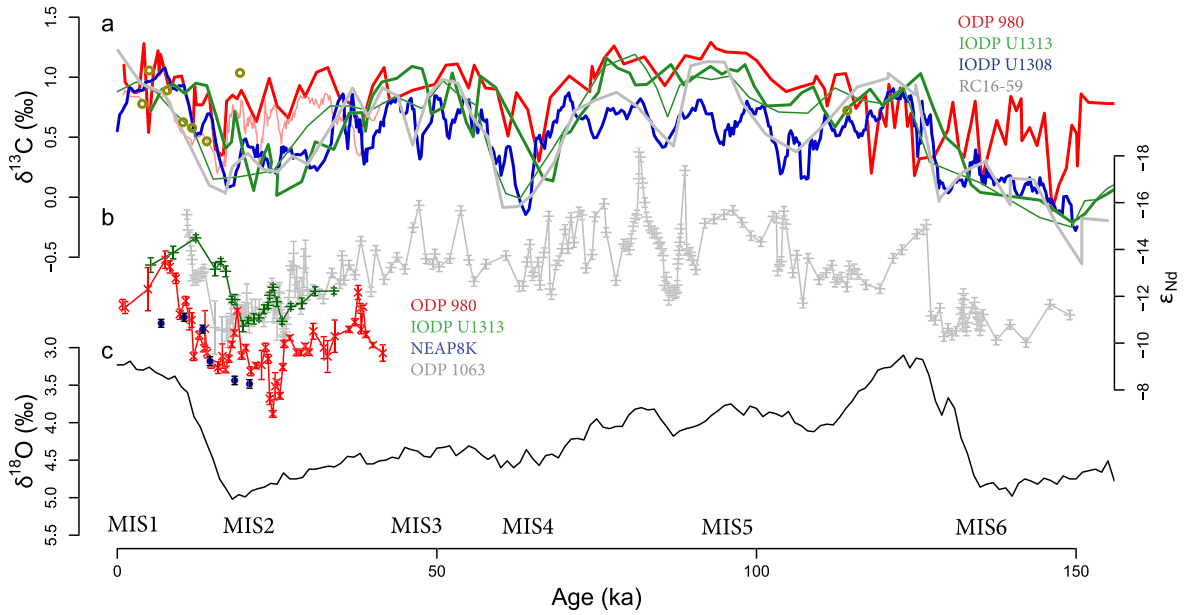

Fig. 2. Carbon isotope and ε_{Nd} profiles from Atlantic Sites. a: carbon isotope data from three sites used in this study and one record from RC16-59 (Broecker et al., 2015), red: 980 (2168 m; McManus et al., 1999), blue: U1313 (3426 m; DSDP 607, Raymo et al., 1989) and dark blue: U1308 (3871 m; Hodell et al., 2008) grey RC16-59 (3500 m). b: ε_{Nd} profiles from sites in similar locations red ODP 980 (Crocker et al., 2016), green IODP 1313 (Lang et al., 2016), blue NEAP8K (Yu et al., 2008) c: LR04 stack oxygen isotope data showing global ice volume and deep sea temperature. Both circulation proxies suggest an expansion of AABW across the basin and up to intermediate depths during the glacial cycle.

ferent glacial solutions, and rely on many mechanisms to lower atmospheric CO_2 (Hain et al., 2010; Kohfeld and Ridgwell, 2013; Martinez-Boti et al., 2015; Skinner, 2009). Similarly, the extent to which sustained northern deep water formation may inhibit the volumetric proportion of AABW (and thus its assumed carbon storage potential) could be crucial to understanding the sensitivity of ocean circulation to large changes in climate (Gebbie, 2014). Most published studies tracing the geometry of NADW over the last 20 kyr and longer have utilised $\delta^{13}C$ in benthic foraminiferal calcite (e.g. Curry and Oppo, 2005). Although this work has greatly improved our understanding of the changing patterns of circulation there is a degree of ambiguity associated with the use of $\delta^{13}C$ in this way. As $\delta^{13}C$ is a non-conservative tracer, its preformed (surface) water signal can be modified during transport to the deep ocean. This is primarily achieved by conservative mixing as well as by the acquisition of organic, remineralised carbon (Lynch-Stieglitz, 2003). In addition, the end member compositions of preformed nutrients and thus, $\delta^{13}C$ likely vary, through time, in particular as a result of variable air–sea gas exchange in the high latitude surface ocean (Lynch-Stieglitz et al., 1995). In the modern ocean Southern sourced water (SSW) is typically characterised by low $\delta^{13}C$ (i.e. rich in preformed phosphate and other nutrients) and occurs at >2500 m depths in the North Atlantic during glacial maxima (Fig. 2a).

An expansion of southern sourced deep water during the glacial is consistent with neodymium (ε_{Nd}) data from the Atlantic (Fig. 2b), where all records appear to shift towards what are typically considered to be southern sourced values of ~ -8 ε_{Nd}, which in sites deeper than 2500 m is also coincident with the $\delta^{13}C$ minima. ε_{Nd} is a more conservative tracer than $\delta^{13}C$, but the potential for ε_{Nd} change in endmembers, particularly in the North Atlantic, complicates the picture; changes in endmember composition could drive change in Nd isotopic composition at all depths even without large circulation changes or mixing of slow moving water masses (Howe et al., 2016, Fig. 2b). Furthermore, while ε_{Nd} tracks deep water source area and pathway, it is not a sensitive proxy for detecting changes to water mass carbon content or changes in transport path without associated changes to water mass geometry or source (Gebbie, 2014; Howe et al., 2016). Other proxies commonly used to establish and deconvolve water mass provenance and flow rates, such as Cd/Ca, Pa/Th and sortable silts can also suffer from ambiguities in their interpretation, due to localised effects or geochemical interactions (e.g. Marchitto, 2013; Thomas et al., 2006). Despite a broad understanding of the potential changing patterns of ocean circulation in the North Atlantic over the last glacial cycle, there is a pressing need for additional proxy based information to reveal the full evolution of ocean circulation with respect to climate over this time interval, particularly in the form of nutrient-type proxies which can trace biological utilisation and the carbon content of the ocean interior.

The boron content and isotopic composition of benthic foraminiferal tests has potential as an additional tracer of deep water circulation and deep water carbon content (Yu et al., 2008; Yu and Elderfield, 2007). The direct link to the carbonate system that underlies both the B/Ca–CO_3^{2-} proxy (Yu and Elderfield, 2007; see below), and the boron isotope-pH proxy (Rae et al., 2011) provides a unique insight into ocean carbon storage, has fewer controlling influences than $\delta^{13}C$, and because the carbonate system is semi-conservative (i.e. is changed through both conservative mixing and internal ocean processes such as respiration and carbonate production), in the modern ocean it also makes a good tracer of water mass structure on an ocean basin scale (see Fig. 1b). Existing boron proxy data suggests that low [CO_3^{2-}] (high CO_2 and hence low pH) water invaded the Atlantic at depths greater than 2800 m during the last glacial cycle around 70 kyrs ago (Yu et al., 2016). As southern sourced water in the Atlantic is known to have remained low in carbonate ion concentration throughout the last glacial period from qualitative measurements (e.g. preservation, Hodell et al., 2001) and chemical proxy measures (e.g. [CO_3^{2-}], Yu et al., 2014), these data are consistent with $\delta^{13}C$-based interpretations of SSW expansion into the deep Atlantic at all latitudes (Fig. 2; Hodell et al., 2008; McManus et al., 1999; Raymo et al., 1989; Sarnthein et al., 1994). During the deglaciation, modern-style circulation resumed as chemical stratification collapsed (Yu et al., 2008), but when and how that stratification first developed across the North Atlantic basin remains uncertain, partly because of the limitations on depth, spatial and temporal coverage of existing

proxies records and partly because of the uncertainties associated with ε_{Nd} and $\delta^{13}C$ proxy reconstructions (Fig. 2).

Here we report records of B/Ca and $\delta^{11}B$ in benthic foraminifera from a series of sites across the North Atlantic Ocean from Ocean Drilling Program (ODP) Sites 980 and 999 and Integrated Ocean Drilling Program (IODP) sites U1313 and U1308. Glacial–interglacial CO_2 change is affected by both changes in water mass geometry and changes to water mass chemical properties, both of which impact on the ocean carbonate system. By utilising a multiproxy approach that incorporates new boron proxy data and combining them with published data from these sites we undertake a more complete examination of this problem that accounts for mixing as well as changes to composition from endmember changes and carbon cycle changes. This allows us to quantify the evolution of carbon storage and ocean circulation in the region over the last glacial cycle.

2. Materials and methods

2.1. Samples and age model

To reconstruct the carbonate system of the deep North Atlantic Ocean over the last glacial cycle, sediment samples were taken from ODP Site 980 (2184 m depth), IODP Site U1313 (3426 m depth) and IODP Site U1308 (3871 m depth) covering the last 150 kyrs. Site 980 was targeted because it is currently bathed in intermediate water sourced from the north (Fig. 1). Sites U1308 and U1313 were chosen because they are currently bathed in NADW, in the eastern and western abyss of the North Atlantic, respectively. New data are also presented from ODP 999 (2839 m depth), a site in the Caribbean Sea currently bathed in Antarctic Intermediate Water (AAIW) because of the shallow sill depth (~1800 m) separating the Caribbean and Atlantic basins (Fig. 1).

The cores studied were already heavily sampled so our samples were taken outside of the primary splices. For Sites 980 and U1308 physical properties (L* and magnetic susceptibility) were then used to tie our sample depths (~10 cm spacing) to the site splices and their appropriate age models (Hodell et al., 2008; McManus et al., 1999).

2.2. Brief analytical and sampling methods

Sediment samples from core material were washed with deionised water and sieved to >63 μm, to separate fine and coarse fractions. Individual foraminifera (Plano-convex specimens of *Cibicidoides wuellerstorfi, sometimes known as Cibicides wuellerstofi, hereafter C. wuellerstorfi*) were hand separated from the 212–500 μm size fraction and measured for boron isotopes and B/Ca ratios using established protocols at the University of Southampton (Henehan et al., 2013; Rae et al., 2011). Detailed methods and carbon system calculations are described in the Supplementary Methods, section 3.

New $\delta^{18}O$ and $\delta^{13}C$ of *C. wuellerstorfii* were generated for Site U1313 and these data are consistent with the sample ages developed in Lang et al. (2016) by tuning this secondary splice to the age model of Naafs et al. (2013) from the primary splice at U1313. All cores are thus tied to the common chronology of the LR04 stack (Lisiecki and Raymo, 2005), the top 40 kyrs of ODP 980 is an exception and uses an updated independent chronology (Crocker et al., 2016). For further details see section 2.3 in the Supplementary Methods.

Hydrographic data for the sites (used for carbonate system calculations) were gathered from the GLODAP dataset (Key et al., 2004), and are presented in Table 1 in the Supplementary Methods.

3. Results

New records of B/Ca and $\delta^{11}B$ data from (I)ODP Sites 980, 999, U1313 and U1308 are shown in Fig. 3. The secular evolution of both the B/Ca and $\delta^{11}B$ records are similar among sites. Given the size of the uncertainty envelopes, the changes in benthic $\delta^{11}B$ appear muted when compared to the precision on each individual data point. Only U1313 shows well resolved changes in $\delta^{11}B$ from Holocene values over the last glacial cycle indicating that long term changes of less than ~0.1 pH units are unlikely to be resolvable in $\delta^{11}B$-pH. In contrast, our more highly resolved B/Ca ratio data, captures orbital changes over the glacial cycle and these are particularly evident at the two deepest water sites (U1313 and U1308).

Despite the larger relative uncertainty on $\delta^{11}B$-pH calculated core top pH and $[CO_3^{2-}]$ data from all sites are in good agreement with measured carbonate data (Lauvset et al., 2016, shown in Table 1, Supplementary material). Thus during the late Holocene there was little variability with depth (characteristically $[CO_3^{2-}]$ ~118 ± 20 μmol/kg, and pH ~7.95 ± 0.05), owing to a NADW bathing all depths (as is the case today). Note that due to the pressure and temperature effects on the $\delta^{11}B$-pH proxy, the depth profile of $\delta^{11}B$ is not equivalent to that of pH (see Fig. 3a vs. 4). The linear transformation of B/Ca to ΔCO_3^{2-} (equation (2), Supplemental material), however ensures that the patterns in the ΔCO_3^{2-} data are very similar to raw B/Ca (Fig. 3b vs. Fig. 4). A comparison of the two data types, despite the limitations of our $\delta^{11}B$-pH record, shows a good agreement (Fig. 4, $r^2 = 0.46$ see Supplemental Fig. 1). This supports the assertion of Yu et al. (2010a) that when used in conjunction, these two B-based proxies represent a powerful proxy toolbox, with the analytically more straightforward B/Ca proxy capable of resolving small and high frequency changes and the more labour intensive $\delta^{11}B$-pH providing a robust framework by which to interpret changes in the ocean carbonate system.

4. Discussion

4.1. Patterns of circulation in the North Atlantic over the last 150 kyr

To reconstruct changing stratification in the North Atlantic over the last glacial cycle, we compare our new estimates of bottom water carbonate ion derived from B/Ca ratios and pH from $\delta^{11}B$ for Sites 980, 999, 1313 and 1308 to existing data from the North Atlantic (Yu et al., 2008), Caribbean Site VM28-122 (3623 m), Ceara Rise (RC16-59; Broecker et al., 2015), and South Atlantic (MD07-3076, Gottschalk et al., 2015, TN057-21, Yu et al., 2014) in a B/Ca time series in Fig. 5 and depth profiles in Fig. 6. Note that for VM28-122, as for Site 999, its location in the Caribbean Sea means that water mass ingression is controlled by sill depth – the effective depth of exchange with the Atlantic is therefore ~1800 m. To first order, the depth-latitude transect of the sites shows that they were all bathed by a high $[CO_3^{2-}]$, high pH water mass (pH ~8 and $[CO_3^{2-}]$ ~120 μmol/kg) during the Eemian (MIS5e) – in a pattern similar to that seen in the Holocene and today (Key et al., 2015) (Fig. 6a and f).

In contrast to the warmest intervals, considerable depth stratification is seen in the carbonate system from MIS2 to MIS5a–d (Fig. 6 panels b–e) with Site 980 at intermediate water depths shifting to higher values in both $[CO_3^{2-}]$ and pH and the deeper sites (U1313 and U1308) showing lower $[CO_3^{2-}]$ and pH. This basic pattern is consistent with several more temporally or spatially restricted compilations (e.g. Yu et al., 2008; Broecker et al., 2015) but we are now able to extend this understanding through a full glacial cycle and across a greater depth range. Our results point to the existence, during cold intervals (LGM, and MISs 4 and 6, Fig. 6 panels

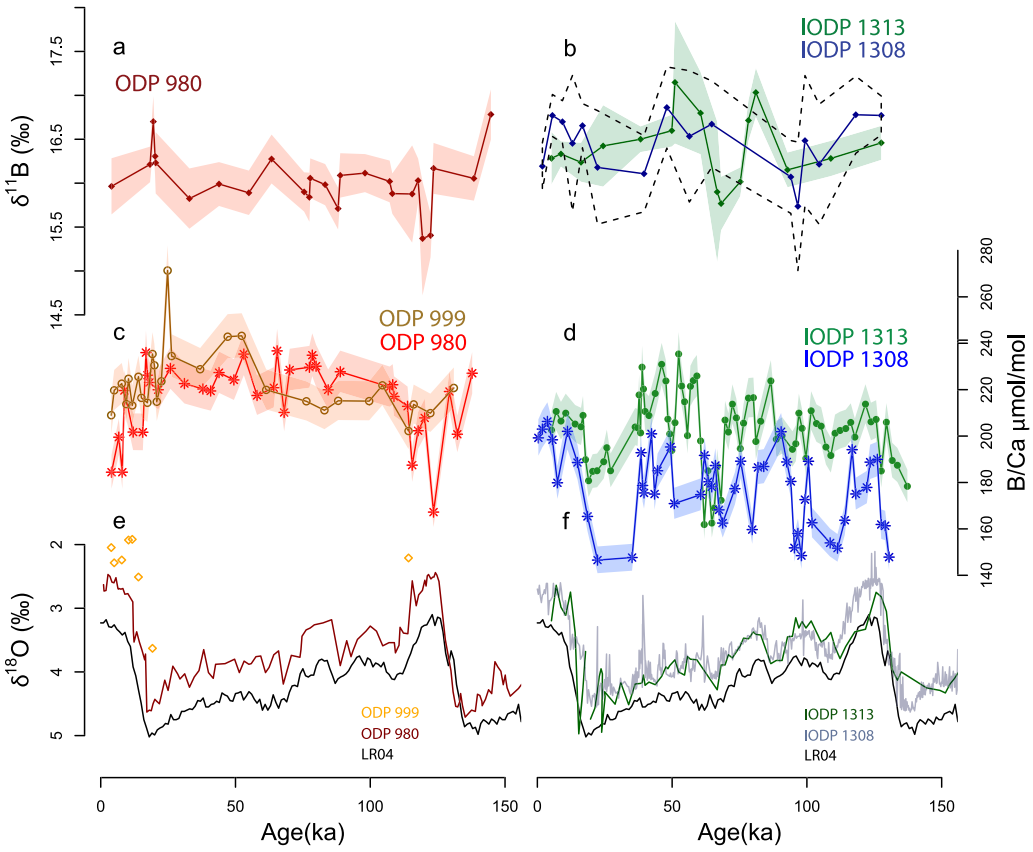

Fig. 3. δ^{11}B and B/Ca data. Boron isotope data from (I)ODP sites, a: red: 980, b: blue: U1313, dark blue: U1308 (dotted uncertainty envelope for clarity). External 2SD uncertainty is shown by the shading and dotted lines. c, d: B/Ca from the same sites and also ODP 999 in the Caribbean (C) revealing more structure due to the higher resolution. e, f: shows the LR04 stack of benthic isotopes (Lisiecki and Raymo, 2005) and Site specific δ^{18}O: ODP 980 (Crocker et al., 2016), IODP U1308 (Hodell et al., 2008) and IODP U1313 (this study).

b, d and g) of an enlarged low-[CO_3^{2-}] deep water mass shoaling to between 2800 and 3400 m – consistent with previous findings based on δ^{13}C and B/Ca for the LGM (Curry and Oppo, 2005; Gebbie, 2014; Yu et al., 2008). These full glacial characteristics, with a strong chemical gradient at ∼2500 m are indicative of greater carbon storage in the deep ocean below a steepened chemocline than during the Holocene.

To a first order the carbonate system appears to be primarily depth-dependent in the North Atlantic, with the western basin (this study, Yu et al., 2010a; Broecker et al., 2015) following the same trends as a compilation of records for the eastern basin (Yu et al., 2008) for a given depth during the last 40 kyr (Fig. 5a and b).

For the last glacial cycle, three distinct "modes" of carbonate system depth stratification are evident, each associated with a characteristic circulation pattern in the Atlantic (Fig. 6) (Broecker et al., 2015; Gottschalk et al., 2015; Yu et al., 2014, 2008). An interglacial "overturning mode", seen during the Holocene and in MIS5e with little vertical structure in [CO_3^{2-}] and pH (LOESS fit lines in Fig. 6, see supplemental materials section 2.3 for details); a "weak glacial stratification mode" with enhanced AABW penetration confined below 3400 m, seen during MIS5a–d and MIS3 (Figs. 6c and 6e); and a "full glacial mode", wherein the interface between northern and southern sourced water is shallowest, situated no deeper than 2800 m in the LGM and MIS4 featuring and the strongest vertical gradients in reconstructed carbonate chemistry (Fig. 6b and 6d).

While both of our deep water sites show reductions in pH and carbonate in the cold periods of the last glacial cycle, the amplitude of change is greater (to lower values) in the eastern basin (Site U1308) than in the western basin (Site U1313), especially during MIS4 and the LGM/MIS2 (Fig. 5). We attribute this observation to the greater depth of Site U1308 (by ∼400 m) and therefore greater influence of AABW.

4.2. Controls on Atlantic carbonate system variations

Although the carbonate system is predominantly quasi-conservative in the modern ocean (see Fig. 1) and its properties strongly determined by water mass source, there is no guarantee that this characteristic of the system is maintained in the geological past. Given that the carbonate system tracers will react differently to δ^{13}C to changes in biological modification and/or carbon flux the two proxy systems can be used together to elucidate both changes in water mass structure/geometry and non-conservative effects (e.g. Yu et al., 2008). Fig. 7 shows a cross plot of δ^{13}C and B/Ca derived [CO_3^{2-}] from (I)ODP Sites 980, 999, U1308 and U1313. During the Holocene (solid circles) and MIS5e all available North Atlantic tracer data cluster around [CO_3^{2-}] ∼120 µmol/kg and δ^{13}C ∼1‰. This is consistent with one water mass bathing all these sites – NADW. Through the glacial cycle the sites diverge with ODP 980 and IODP U1308 following a trend line indicative of CO_2 efflux (ODP 980) and influx (IODP U1308, dashed blue "CO_2 evasion" line). This suggests that at these two East Atlantic Sites the carbonate system remains a quasi-conservative tracer over the glacial cycle, suited to identifying the influence of shallow, well-ventilated GNAIW and deep, isolated AABW respectively in this basin. At Site 980 (considered our northern endmember), glacial pH also increased as expected from lower atmospheric CO_2 and a rapidly ventilated and shallow overturning cell (Fig. 4a). U1308 on the other hand shows no significant pH change in our record,

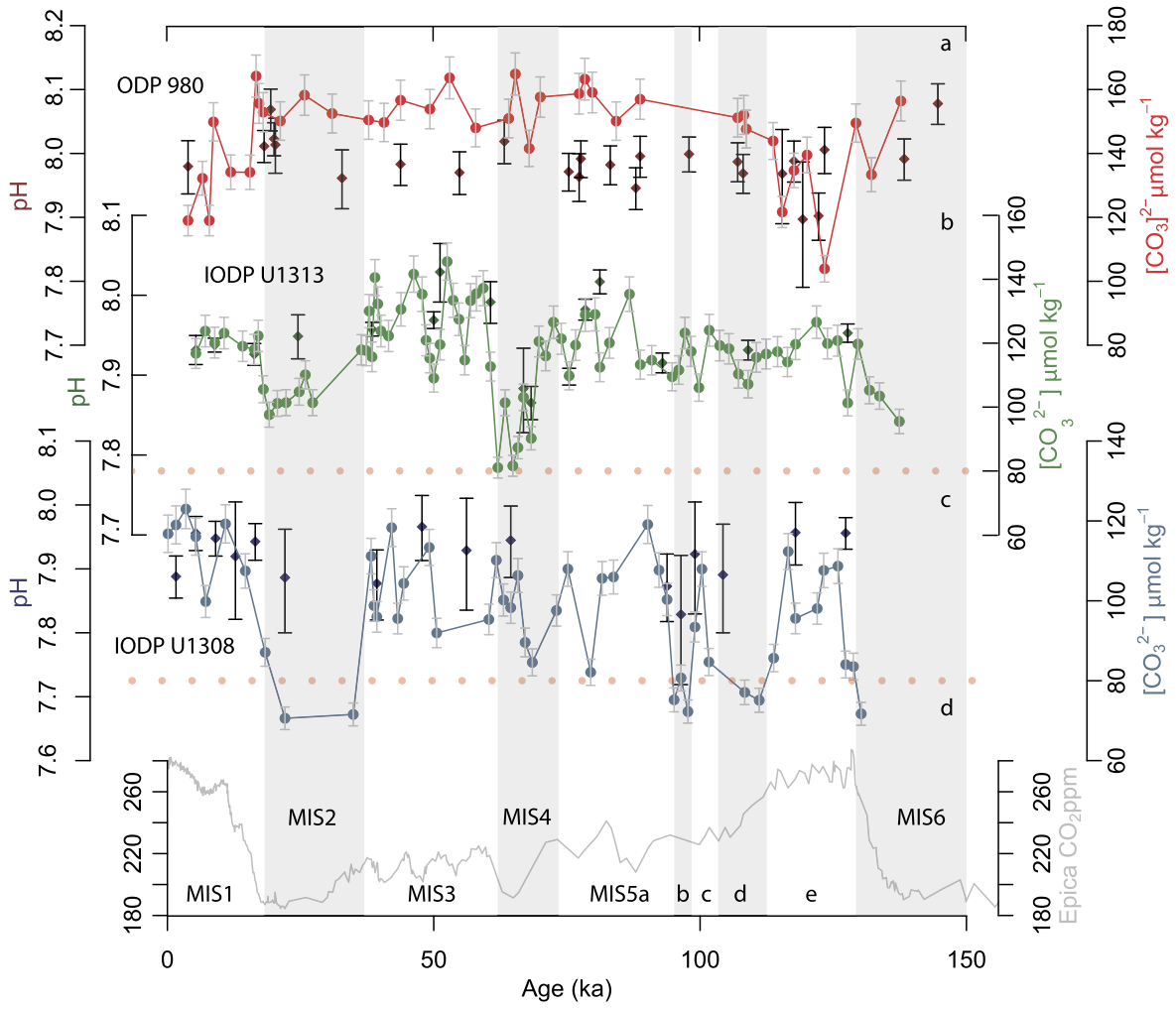

Fig. 4. pH and carbonate data from individual Sites. Paired pH (total scale) and carbonate data from a: ODP 980, b: IODP U1313 and c: IODP U1308. d: Ice core CO_2 (Bereiter et al., 2015). In all sites the pH and carbonate reconstruction follow similar patterns adding confidence to the use of B/Ca as a carbonate proxy, although the pH data does not always have the required resolution to show the smaller changes revealed by the higher resolution B/Ca. Deep water on both sides of the Atlantic reaches SSW compositions of $[CO_3^{2-}]$ at times during the glacial cycle. Shallower sites record high carbonate, high pH intermediate water throughout the glacial period. All diamonds = boron isotope derived pH and external 2SD, all circles = independent B/Ca derived $[CO_3^{2-}]$ and external 2SD.

but without a southern pH-endmember this is impossible to interpret (either as mixing, SSW or accumulation of respired carbon). We therefore limit most of our interpretation at this stage to the B/Ca-$[CO_3^{2-}]$ record alone, which shows well resolved variation.

At U1313, the gradient in δ^{13}C-$[CO_3^{2-}]$ space is significantly steeper than the trend seen at U1303 and 980, representing much less conservative behaviour, as seen from the larger range of δ^{13}C values. This evolution through the last glacial cycle shows that U1313 is either influenced by a change in southern sourced end-member composition (black diamond, in Fig. 7; Gottschalk et al., 2015; Yu et al., 2014) or exhibits an increased build-up of remineralized carbon along the water pathway (shown by black dashed 'biology' line, after Yu et al., 2008). U1313 also shows the largest resolvable changes through time in δ^{11}B-pH (Fig. 4), which may also signal accumulation of extra carbon in the local deep water. This behaviour is most likely attributable to southern sourced water mass divergence north of the Romanche and Vema fracture zones before reaching sites U1313 and U1308. Our δ^{13}C data point to a build-up of remineralized carbon in the western basin relative to the eastern basin. Although other processes may be contributory (e.g. carbonate compensation), these combined data sets suggest that both a change in water mass geometry and differential acquisition of carbon in eastern and western basins are required to explain the carbonate system patterns we have reconstructed over the last glacial cycle in the deep Atlantic Ocean.

4.3. Atlantic carbonate system depth stratification linked to CO_2 storage

In order to examine the temporal evolution of stratification of the carbonate system in the North Atlantic basin we define and plot a stratification index $[CO_3^{2-}]^*$: the difference between $[CO_3^{2-}]$ at Site 980 ($[CO_3^{2-}]_{980}$) and the available deep water sites ($([CO_3^{2-}]_{980} - [CO_3^{2-}]_{U1313,\,U1308\text{ and RC16-59}}$); Fig. 8). Site 980, is interpreted to have been continually bathed in northern-sourced waters during both glacials and interglacials throughout the Late Pleistocene (Fig. 7 and Raymo et al., 1990). $[CO_3^{2-}]^*$ is then interpreted as the relative influence of northern and southern sourced waters in the deep part of the basin and/or the relative increase in respired carbon storage. High values of $[CO_3^{2-}]^*$ are therefore associated with enhanced carbonate system stratification between shallow and deep, and/or increased deep ocean carbon storage. Deep water entering the South Atlantic from either the Southern Ocean or the Pacific has a low $[CO_3^{2-}]$ composition such as shown at sites TN057-21 at 41°S, 7.8°E 4981 m and MD07_3076 at 44°S, 14°W, 3770 m (Gottschalk et al., 2015; Yu et al., 2014), which is also true of Pacific Ocean water, as seen

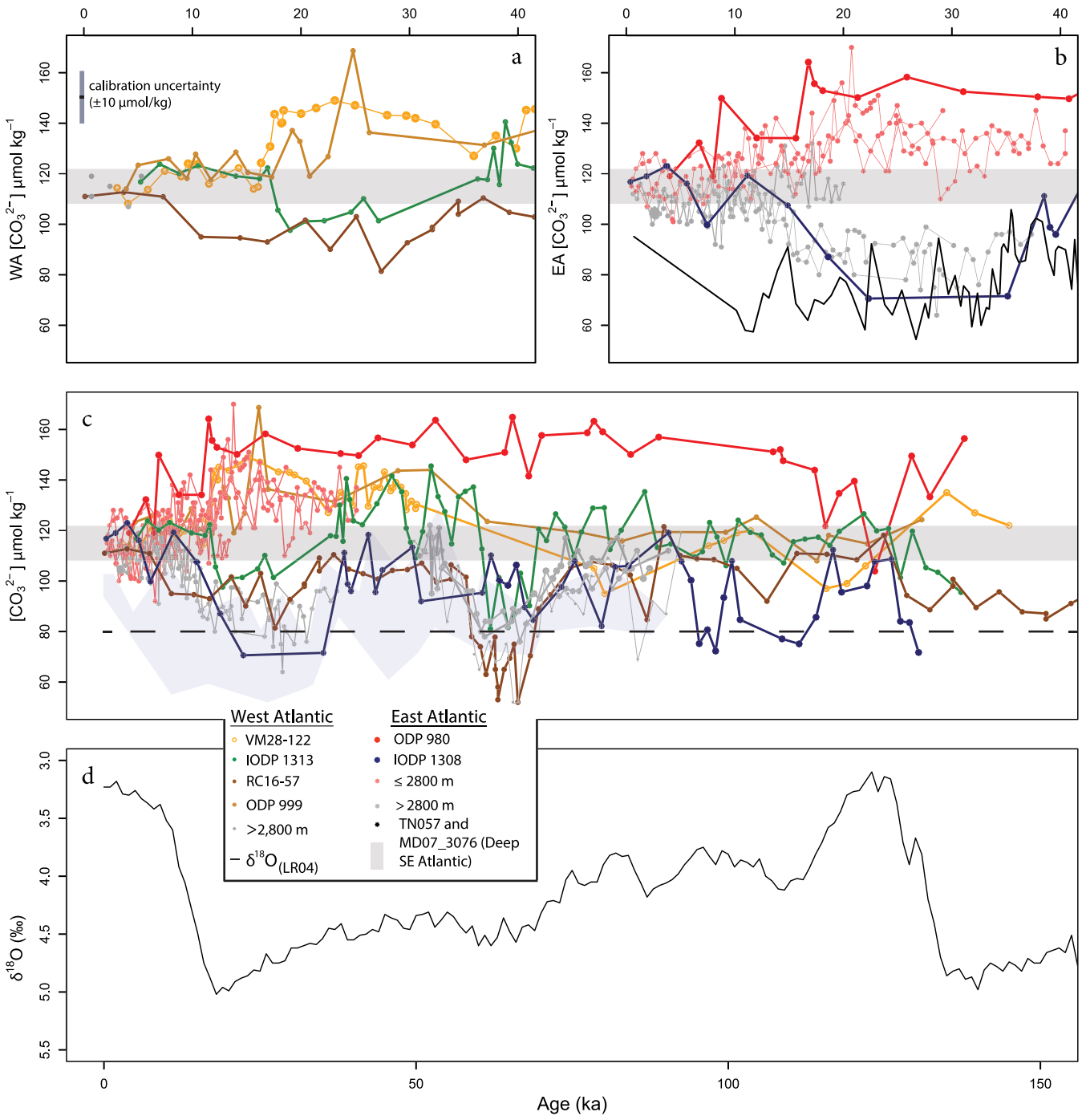

Fig. 5. [CO_3^{2-}] gradients in the North Atlantic. a: B/Ca derived-[CO_3^{2-}] concentration from the West Atlantic Basin, VM28-122 (Yu et al., 2010b), IODP 1313 and RC16-59 (Broecker et al., 2015). b: compilation from the Eastern Atlantic basin, ODP 980, IODP 1308, other sites <2800 m pale red, pale grey >2800 m (BOFS and NEAPS Sites from Yu et al., 2008), black, South Atlantic (Gottschalk et al., 2015; Yu et al., 2014) c: 150 kyrs of data from the whole Atlantic basin (see above for colour scheme), the grey bars in a–c show modern Atlantic deep water composition, and the dotted line indicated modern southern sourced water composition. Pale shading indicates the range of values from the South Atlantic TN057 and MD07_3076 (Gottschalk et al., 2015). d: LR04 for glacial–interglacial reference (Lisiecki and Raymo, 2005). Shallow sites form an upper, high carbonate cell during the LGM and deeper sites a low carbonate cell. Depth stratification is eroded following the resumption of a strong AMOC following the last deglaciation (panels a and b) and the penultimate deglaciation (panel c).

by site RR0503-83 (Allen et al., 2015), see yellow oval in Fig. 7. Any excursion to higher values of [CO_3^{2-}]* (the down direction on Figs. 8 and 9), marks an increase in carbonate system stratification of the basin and greater influence of low [CO_3^{2-}] waters at depth. We characterise this low [CO_3^{2-}] water as having a southern source, particularly evident in the eastern Atlantic basin, with low $\delta^{13}C$, very low [CO_3^{2-}] and potential low pH (i.e. a relatively high DIC water mass). This strong influence of SSW influence at depth is evident from MIS5a–d through MIS2, with the most prominent intervals being MIS2, MIS4, MIS5d and MIS6 where deep water [CO_3^{2-}] is between 40 and 90 µmol/kg lower than northern sourced water (NSW) values (solid diamonds in Fig. 7, and Fig. 8). In the western Atlantic basin, the steeper gradient of $\Delta\delta^{13}C$ to Δ[CO_3^{2-}] seen in Fig. 7 strongly implicates remineralized, biologically utilised carbon as being the driver of the lower [CO_3^{2-}]* of this basin.

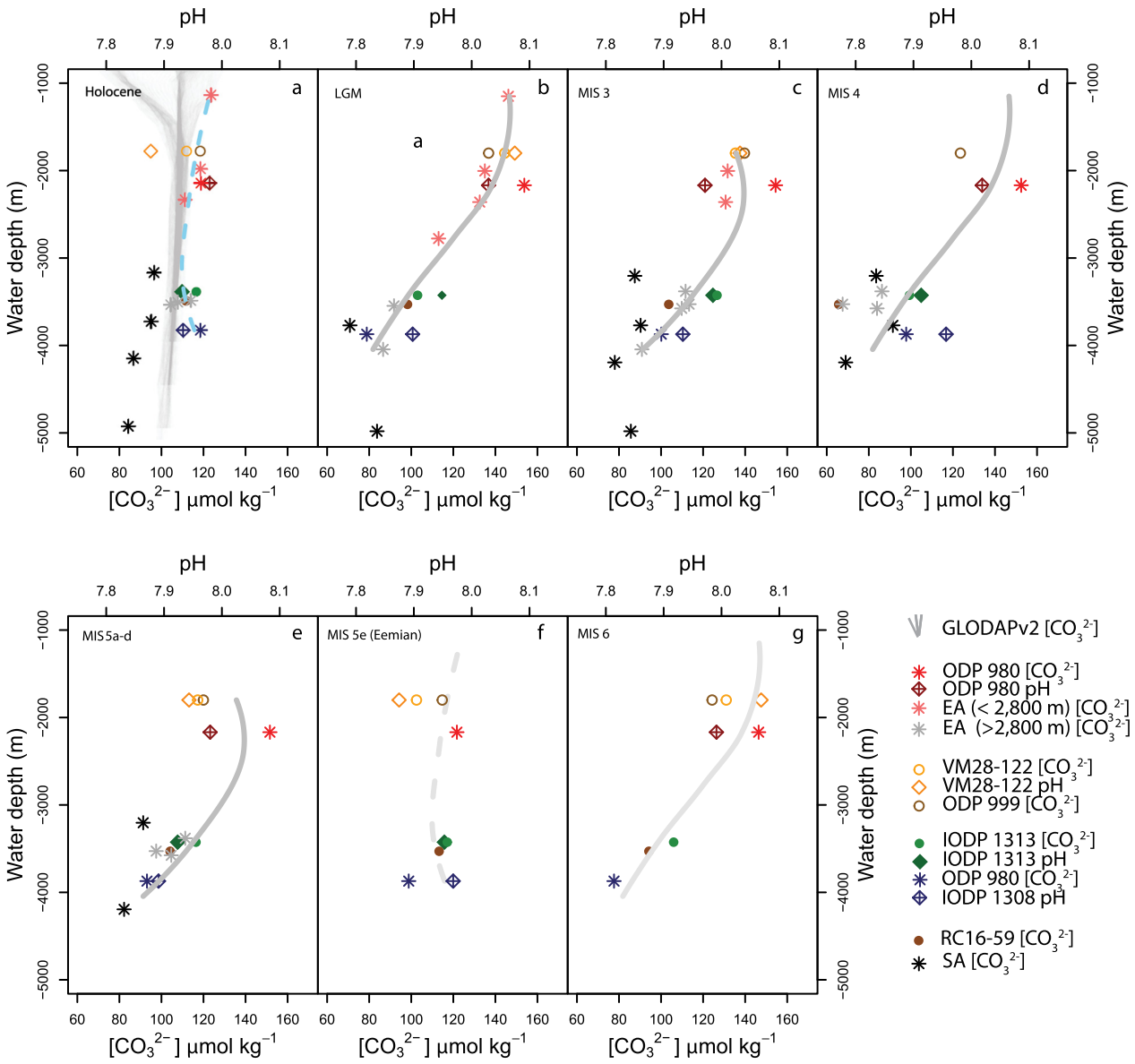

Fig. 6. Carbonate system depth profiles from the North Atlantic. Depth profiles from data generated here and published B/Ca-$[CO_3^{2-}]$ and δ^{11}B-pH data in the Atlantic including all sites from Fig. 5 and this study. Solid circles and stars show carbonate ion data (West and East Atlantic respectively), solid and crossed diamonds show pH data (WA and EA respectively), Caribbean Sites VM28-122 (Yu et al., 2010b) and ODP 999 are plotted at an effective depth of 1800 m (denoted by an open symbol). a: Modern and Holocene (0–6 kyrs) $[CO_3^{2-}]$ profile, grey lines show Modern North Atlantic hydrography from the GLODAP dataset. A loess best fit is provided for the B/Ca-$[CO_3^{2-}]$ data (blue dotted line). b: LGM (18–25 kyrs) the fitted line (as Holocene) shows a distinct chemocline between deep and shallow sites (~3,000 m) with deeper sites showing depletion in carbonate ion with shallower sites being enriched. c: MIS3 (31–55 kyrs) shows broadly intermediate characteristics between full interglacial (a, f) and full glacial (b, d), with mid depth sites showing higher $[CO_3^{2-}]$. d: MIS4 (59–69 kyrs) similar distribution of carbonate ion and pH to the LGM (b). e: MIS5a–d (82–109 kyrs) similar characteristics to MIS3 (c). F: MIS5e (118–128 kyrs) The peak of the last interglacial appears similar in nature to the Holocene (a) despite fewer data, and is presented with the Holocene best fit line. g: MIS6 (130–150 kyrs) data points, similar in nature to the LGM and shown with the LGM best fit line. The local regression (loess) lines fitted on the $[CO_3^{2-}]$ data were calculated in the R statistical software, using a smoothing function which takes account of all depths but with decreasing weighting according to the cube of their distance in the depth domain (for more details see supplemental information section 3.3), we use data from the Holocene, MIS2 and MIS3 for these lines and apply them to other time slices which share 'modes' of circulation.

The temporal evolution of carbonate ion stratification in the North Atlantic bears some similarity to the depth stratification of $\delta^{13}C$ ($\Delta\delta^{13}C$, Fig. 8a). However, there are more resolvable differences in $\Delta[CO_3^{2-}]$ than in $\Delta\delta^{13}C$ between the sites especially during the MIS3 and 5a–d. The carbonate ion gradient plot suggests strong stratification throughout much of the last glacial cycle as opposed to merely during MIS2 and MIS4 as suggested by $\Delta\delta^{13}C$ (Fig. 8b). The $[CO_3^{2-}]$ and $\delta^{13}C$ data are complementary for the most-part, but minor or short-lived SSW excursions may be more easily resolved in the $[CO_3^{2-}]$ dataset because they will form a larger relative change. Regardless of processes represented in the proxy values, there is a good correlation between $[CO_3^{2-}]^*$ in the deep north Atlantic cores and atmospheric CO_2 (Fig. 9, cross-correlation (r^2) of 0.59, similar to the 0.46 from Southern Ocean $\Delta\delta^{13}C$, Hodell et al., 2003). This correlation supports a contribution to CO_2 change throughout the last glacial cycle by changes in the stratification of the carbonate system in the Atlantic resulting from the expansion of the SSW cell. The residual ($[CO_3^{2-}]^*$ not contributing to CO_2 change) is shown in the lower panel of Fig. 9, and at lower CO_2 (glacial) values is generally close to analytical precision (<10 µmol/kg) and thus insignificant. At higher CO_2 levels (interglacial), the $[CO_3^{2-}]^*$ residual increases to >20 µmol/kg, implying that the $[CO_3^{2-}]^*$:CO_2 relationship is a less important process during high CO_2 periods. This is perhaps indicative of

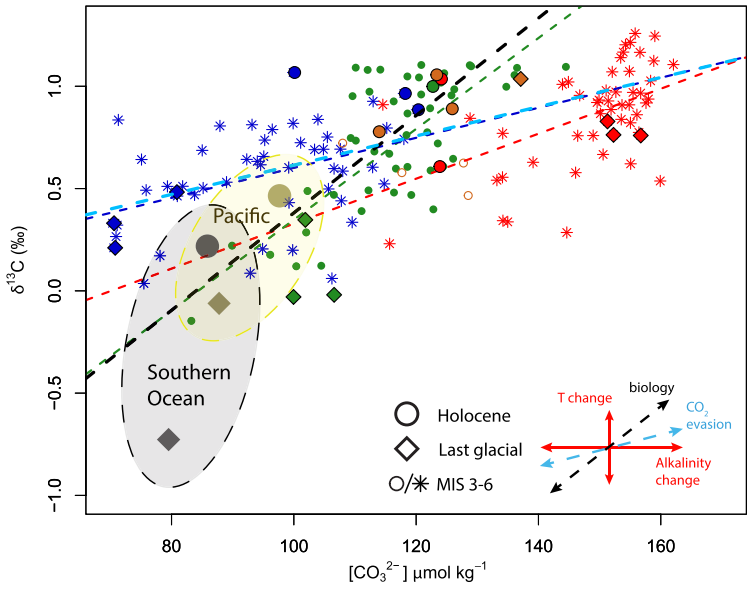

Fig. 7. $\delta^{13}C$: $[CO_3^{2-}]$ cross plot. B/Ca derived carbonate data and co-occurring $\delta^{13}C$ data from ODP 980 (red stars), IODP U1313 (green circles), IODP U1308 (dark blue stars) and ODP 999 (dark yellow hollow circles). Also shown are shaded endmember compositions for the Southern Ocean (grey oval, Yu et al., 2014) and the Pacific (yellow oval, Kerr et al., 2017). Holocene and last glacial data are highlighted by solid points (black-bordered circles and diamonds respectfully), the glacial northern endmember is assumed to be denoted by the cluster of glacial ODP 980 points in the upper-right corner. Linear fit lines are shown for ODP 980, IODP U1313, and IODP U1308 (solid coloured lines) and calculated lines for CO_2 addition/evasion (pale blue, dotted) and biological utilization (black, dotted). Sample gradients for alkalinity and temperature change are also shown, after Yu et al. (2008).

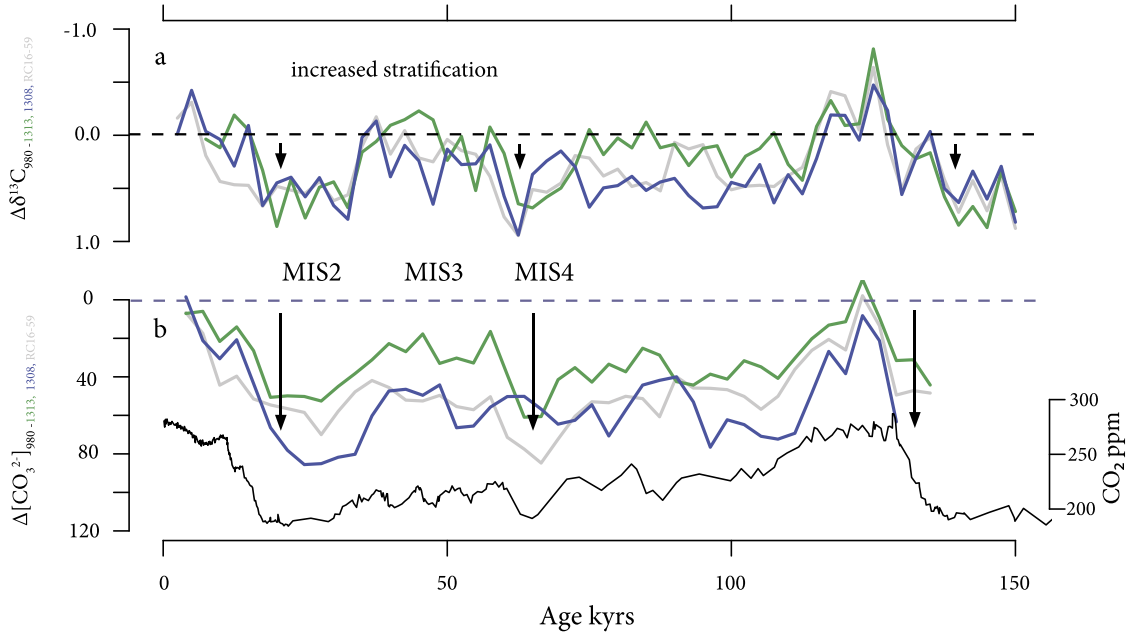

Fig. 8. $\Delta\delta^{13}C$ and $\Delta[CO_3^{2-}]$, controls on CO_2. a: The difference between NSW end member (980) and the three deeper sites U1313 (green), U1308 (dark blue) and RC16-59 (grey), as $\Delta\delta^{13}C$ ($\delta^{13}C_{980}-\delta^{13}C_{SITE}$) and b: $\Delta[CO_3^{2-}]$ calculated by $[CO_3^{2-}]_{980}-[CO_3^{2-}]_{SITE}$. $\Delta[CO_3^{2-}]$ is largest at U1308 particularly during times of maximum CO_2 decline shown in panel b, suggesting the deep East Atlantic is an important reservoir for C-storage. The shape of the $\delta^{13}C$ and $\Delta[CO_3^{2-}]$ stratification bears striking resemblance to CO_2 (lower panel b). The two cores in the western basin (U1313 and RC16-59) show variable stratification with the deeper and more southerly core (RC16-59) being further from the northern end member at all times (and thus showing greater influence of SSW).

other non-Atlantic processes dominating the relatively minor CO_2 changes in the Holocene and MIS5. Furthermore, during glacial onset U1308 shows a large change in $[CO_3^{2-}]^*$ but generally has a weaker correlation to CO_2 over the whole cycle than the West Atlantic ($r^2 = 0.38$ and 0.62 respectively). During termination 1 (and 2) both eastern and western basin $[CO_3^{2-}]^*$ indices show a strong relationship with CO_2 as would be expected from the large and fast collapse in the deep ocean carbon storage reservoir that occurred at these times.

5. Conclusions

Using relatively low temporal resolution $\delta^{11}B$ data combined with higher resolution B/Ca, we find that we can divide Atlantic circulation change throughout the last glacial cycle into three main modes: (i) An interglacial "overturning mode", seen in the Holocene and MIS5e; (ii) a "weak glacial mode" with enhanced AABW penetration confined to below 3400 m, seen in MIS5a–d and MIS3, with a well ventilated circulation in the upper cell, shown by

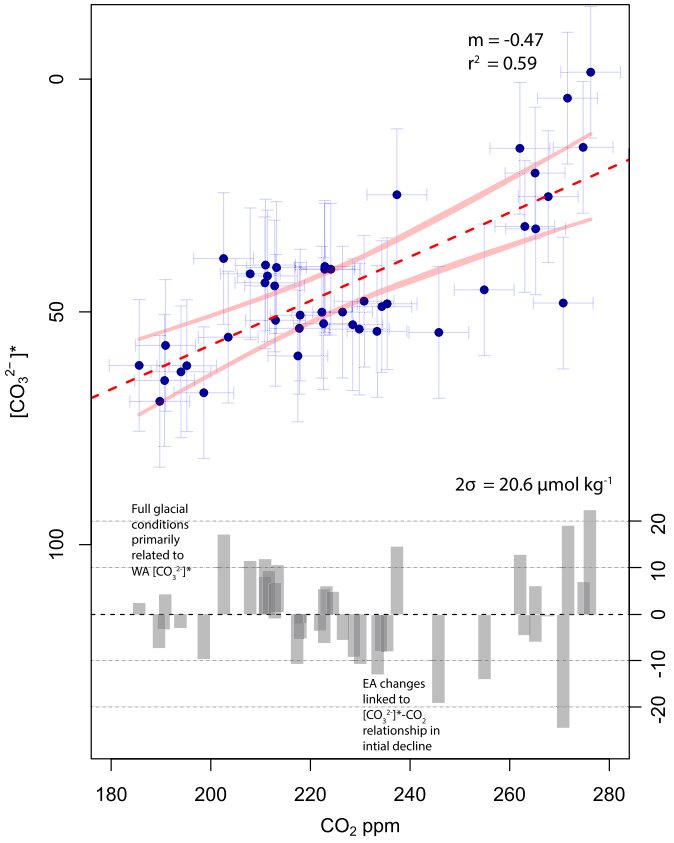

Fig. 9. $[CO_3^{2-}]^*$:CO_2 cross-plot. A cross plot of atmospheric CO_2 from the ice core compilation (Bereiter et al., 2015) against $[CO_3^{2-}]^*$ ($[CO_3^{2-}]_{980} - \frac{([CO_3^{2-}]_{1313}+[CO_3^{2-}]_{1308})}{2}$), shows a correlation, suggesting the deep Atlantic is an important C-store at least partially moderating G–IG CO_2 change, the gradient is −0.47. The $r = 0.77$ ($r^2 = 0.59$) is similar, but greater than that found from $\delta^{13}C$ gradients, overall the western Atlantic $[CO_3^{2-}]^*$ (1313) has a better correlation with CO_2 than the eastern Atlantic (1308, $r^2 = 0.62$ vs. 0.38). The residuals from this relationship are shown in the lower panel. All values are <25 µmol kg^{-1} (2SD = 20.6 µmol kg^{-1}), which is similar in size to the square root addition of analytical and calibration uncertainty of 2 individual measurements (14.1 µmol kg^{-1}), although there is an increase towards higher CO_2 values suggested that deep ocean processes are less strongly linked to interglacial climate states.

high carbonate ion and high pH at a depth of ∼2200 m; and (iii) a "full glacial mode", with the interface between NSW and SSW at no less than 2800 m in the LGM and MIS4.

It is likely that CO_2 drawn down into the surface Southern Ocean during cold intervals and stored in an expanded deep ocean southern sourced cell was a quantitatively important process (Fig. 5). This hypothesis is well supported by the correlation observed between atmospheric CO_2 and deep ocean carbonate parameters in the North Atlantic (Fig. 9), and hence the increased volume of high DIC low $[CO_3^{2-}]$ water. In addition we find that changes in the eastern basin occur early in the glacial cycle, alongside the stadial–interstadial changes in MIS5. The western basin $[CO_3^{2-}]$ content exhibits greater correlation with atmospheric CO_2 during the coldest intervals compared to the eastern basin as the water there appears to accumulate more respired carbon. Improved spatial coverage of data from all ocean basins is however needed to further investigate this pattern and to better understand the capacity of the oceans to drawdown and release of carbon, a process of key importance for ocean–atmosphere interactions in our warming future. Boron-based proxies demonstrate semi-conservative behaviour over the last glacial cycle which, in concert with either non-conservative or fully conservative tracers such and $\delta^{13}C$ and ε_{Nd}, makes them a powerful constraint on the results and mechanisms of carbon cycle change.

Acknowledgements

We are grateful to Walter Hale and the staff at the Bremen core repository and the (I)ODP, for providing sample material. Thanks to Ian Bailey, Anya Crocker, Dave Lang, Erin McClymont, and Rachael James for discussion and comments on various forms of this work. We also thank Eleanor Evetts, Megan Spencer, Andy Milton, Matt Cooper, and Agnes Michalik and well as the rest of the Foster lab for laboratory assistance. We also thank Jess Adkins and two anonymous reviewers for their insightful comments on this submission. This research was supported by NERC studentship number NE/I528626/1 to T.B.C. and NERC grant NE/D00876X/2 and NE/H006273/1 to G.L.F. and NE/F00141X/1 to P.A.W. and a Royal Society Wolfson Research Merit Award to P.A.W.

Appendix A. Supplementary material

Supplementary material related to this article can be found online at https://doi.org/10.1016/j.epsl.2018.12.022.

References

Ahn, J., Brook, E.J., 2008. Atmospheric CO_2 and climate on millennial time scales during the last glacial period. Science 322, 83–85.
Allen, K.A., Sikes, E.L., Hönisch, B., Elmore, A.C., Guilderson, T.P., Rosenthal, Y., Anderson, R.F., 2015. Southwest Pacific deep water carbonate chemistry linked to high southern latitude climate and atmospheric CO_2 during the last glacial termination. Quat. Sci. Rev. 122, 180–191.
Archer, D., Winguth, A., Lea, D., Mahowald, N., 2000. What caused the glacial/interglacial atmospheric pCO_2 cycles? Rev. Geophys. 38, 159–189.
Bereiter, B., Eggleston, S., Schmitt, J., Nehrbass-Ahles, C., Stocker, T.F., Fischer, H., Kipfstuhl, S., Chappellaz, J., 2015. Revision of the EPICA Dome C CO_2 record from 800 to 600 kyr before present. Geophys. Res. Lett. 42, 542–549.
Böhm, E., Lippold, J., Gutjahr, M., Frank, M., Blaser, P., Antz, B., Fohlmeister, J., Frank, N., Andersen, M., Deininger, M., 2015. Strong and deep Atlantic meridional overturning circulation during the last glacial cycle. Nature 517, 73.
Broecker, W.S., Denton, G.H., 1989. The role of ocean–atmosphere reorganizations in glacial cycles. Geochim. Cosmochim. Acta 53, 2465–2501.
Broecker, W.S., Yu, J., Putnam, A.E., 2015. Two contributors to the glacial CO_2 decline. Earth Planet. Sci. Lett. 429, 191–196.
Brovkin, V., Ganopolski, A., Archer, D., Munhoven, G., 2012. Glacial CO_2 cycle as a succession of key physical and biogeochemical processes. Clim. Past 8, 251–264.
Burke, A., Robinson, L.F., 2012. The Southern Ocean's role in carbon exchange during the last deglaciation. Science 335, 557–561.
Crocker, A.J., Chalk, T.B., Bailey, I., Spencer, M.R., Gutjahr, M., Foster, G.L., Wilson, P.A., 2016. Geochemical response of the mid-depth Northeast Atlantic Ocean to freshwater input during Heinrich events 1 to 4. Quat. Sci. Rev. 151, 236–254.
Crowley, T.J., 2000. CLIMAP SSTs re-revisited. Clim. Dyn. 16, 241–255.
Curry, W.B., Oppo, D.W., 2005. Glacial water mass geometry and the distribution of delta C-13 of Sigma CO_2 in the western Atlantic Ocean. Paleoceanography 20.
Gebbie, G., 2014. How much did Glacial North Atlantic Water shoal? Paleoceanography 29, 190–209.
Gottschalk, J., Skinner, L.C., Misra, S., Waelbroeck, C., Menviel, L., Timmermann, A., 2015. Abrupt changes in the southern extent of North Atlantic Deep Water during Dansgaard–Oeschger events. Nat. Geosci. 8, 950–954.
Grant, K.M., Rohling, E.J., Ramsey, C.B., Cheng, H., Edwards, R.L., Florindo, F., Heslop, D., Marra, F., Roberts, A.P., Tamisiea, M.E., Williams, F., 2014. Sea-level variability over five glacial cycles. Nat. Commun. 5.
Hain, M.P., Sigman, D.M., Haug, G.H., 2010. Carbon dioxide effects of Antarctic stratification, North Atlantic Intermediate Water formation, and subantarctic nutrient drawdown during the last ice age: diagnosis and synthesis in a geochemical box model. Glob. Biogeochem. Cycles 24, GB4023.
Henehan, M.J., Rae, J.W., Foster, G.L., Erez, J., Prentice, K.C., Kucera, M., Bostock, H.C., Martínez-Botí, M.A., Milton, J.A., Wilson, P.A., 2013. Calibration of the boron isotope proxy in the planktonic foraminifera *Globigerinoides ruber* for use in palaeo-CO_2 reconstruction. Earth Planet. Sci. Lett. 364, 111–122.
Hodell, D.A., Channell, J.E.T., Curtis, J.H., Romero, O.E., Rohl, U., 2008. Onset of "Hudson Strait" Heinrich events in the eastern North Atlantic at the end of the middle Pleistocene transition (similar to 640 ka)? Paleoceanography, pa4218. https://doi.org/10.1029/2008pa001591.
Hodell, D.A., Kanfoush, S.L., Shemesh, A., Crosta, X., Charles, C.D., Guilderson, T.P., 2001. Abrupt cooling of Antarctic surface waters and sea ice expansion in the South Atlantic sector of the Southern Ocean at 5000 cal yr BP. Quat. Res. 56, 191–198.
Hodell, D.A., Venz, K.A., Charles, C.D., Ninnemann, U.S., 2003. Pleistocene vertical carbon isotope and carbonate gradients in the South Atlantic sector of the Southern Ocean. Geochem. Geophys. Geosyst. 4, 1–19.

Howe, J.N.W., Piotrowski, A.M., Noble, T.L., Mulitza, S., Chiessi, C.M., Bayon, G., 2016. North Atlantic deep water production during the Last Glacial Maximum. Nat. Commun. 7, 11765.

Kerr, J., Rickaby, R., Yu, J., Elderfield, H., Sadekov, A.Y., 2017. The effect of ocean alkalinity and carbon transfer on deep-sea carbonate ion concentration during the past five glacial cycles. Earth Planet. Sci. Lett. 471, 42–53.

Key, R.M., Kozyr, A., Sabine, C., Lee, K., Wanninkhof, R., Bullister, J., Feely, R., Millero, F., Mordy, C., Peng, T.-H., 2004. A global ocean carbon climatology: results from Global Data Analysis Project (GLODAP). Glob. Biogeochem. Cycles 18, GB4031.

Key, R.M., Olsen, A., van Heuven, S., Lauvset, S.K., Velo, A., Lin, X., Schirnick, C., Kozyr, A., Tanhua, T., Hoppema, M., 2015. Global Ocean Data Analysis Project, Version 2 (GLODAPv2). ORNL/CDIAC-162, NDP-093.

Kohfeld, K.E., Ridgwell, A., 2013. Glacial–Interglacial Variability in Atmospheric CO_2, Surface Ocean–Lower Atmosphere Processes. American Geophysical Union, pp. 251–286.

Lang, D.C., Bailey, I., Wilson, P.A., Chalk, T.B., Foster, G.L., Gutjahr, M., 2016. Incursions of southern-sourced water into the deep North Atlantic during late Pliocene glacial intensification. Nat. Geosci. 9, 375–379.

Lauvset, S.K., Key, R.M., Olsen, A., van Heuven, S., Velo, A., Lin, X., Schirnick, C., Kozyr, A., Tanhua, T., Hoppema, M., 2016. A new global interior ocean mapped climatology: the $1^\circ \times 1^\circ$ GLODAP version 2. Earth Syst. Sci. Data 8, 325–340.

Lisiecki, L.E., Raymo, M.E., 2005. A Pliocene–Pleistocene stack of 57 globally distributed benthic $\delta^{18}O$ records. Paleoceanography 20, PA1003.

Lynch-Stieglitz, J., 2003. Tracers of past ocean circulation. In: The Oceans and Marine Geochemistry. In: Treatise on Geochemistry, vol. 6, pp. 433–451.

Lynch-Stieglitz, J., Stocker, T.F., Broecker, W.S., Fairbanks, R.G., 1995. The influence of air–sea exchange on the isotopic composition of oceanic carbon: observations and modeling. Glob. Biogeochem. Cycles 9, 653–665.

Marchitto, T.M., 2013. Paleoceanography, physical and chemical proxies| nutrient proxies. In: Mock, C.J. (Ed.), Encyclopedia of Quaternary Science, second edition. Elsevier, Amsterdam, pp. 899–906.

Martinez-Boti, M.A., Marino, G., Foster, G.L., Ziveri, P., Henehan, M.J., Rae, J.W.B., Mortyn, P.G., Vance, D., 2015. Boron isotope evidence for oceanic carbon dioxide leakage during the last deglaciation. Nature 518, 219–222.

McManus, J.F., Oppo, D.W., Cullen, J.L., 1999. A 0.5-million-year record of millennial-scale climate variability in the North Atlantic. Science 283, 971–975.

Naafs, B.D.A., Hefter, J., Grützner, J., Stein, R., 2013. Warming of surface waters in the mid-latitude North Atlantic during Heinrich events. Paleoceanography. https://doi.org/10.1029/2012pa002354.

Rae, J.W., Foster, G.L., Schmidt, D.N., Elliott, T., 2011. Boron isotopes and B/Ca in benthic foraminifera: proxies for the deep ocean carbonate system. Earth Planet. Sci. Lett. 302, 403–413.

Rae, J.W.B., Burke, A., Robinson, L.F., Adkins, J.F., Chen, T., Cole, C., Greenop, R., Li, T., Littley, E.F.M., Nita, D.C., Stewart, J.A., Taylor, B.J., 2018. CO_2 storage and release in the deep Southern Ocean on millennial to centennial timescales. Nature 562, 569–573.

Raymo, M., Ruddiman, W., Backman, J., Clement, B., Martinson, D., 1989. Late Pliocene variation in Northern Hemisphere ice sheets and North Atlantic deep water circulation. Paleoceanography 4, 413–446.

Raymo, M., Ruddiman, W., Shackleton, N., Oppo, D., 1990. Evolution of Atlantic–Pacific $\delta^{13}C$ gradients over the last 2.5 m.y. Earth Planet. Sci. Lett. 97, 353–368.

Raymo, M.E., Oppo, D.W., Flower, B.P., Hodell, D.A., McManus, J.F., Venz, K.A., Kleiven, K.F., McIntyre, K., 2004. Stability of North Atlantic water masses in face of pronounced climate variability during the Pleistocene. Paleoceanography. https://doi.org/10.1029/2003pa000921.

Sarnthein, M., Winn, K., Jung, S.J.A., Duplessy, J.-C., Labeyrie, L., Erlenkeuser, H., Ganssen, G., 1994. Changes in East Atlantic Deepwater Circulation over the last 30,000 years: eight time slice reconstructions. Paleoceanography 9, 209–267.

Schlitzer, R., 2009. Ocean Data View.

Sigman, D.M., Hain, M.P., Haug, G.H., 2010. The polar ocean and glacial cycles in atmospheric CO_2 concentration. Nature 466, 47–55.

Skinner, L.C., 2009. Glacial–interglacial atmospheric CO_2 change: a possible "standing volume" effect on deep-ocean carbon sequestration. Clim. Past 5, 537–550.

Thomas, A.L., Henderson, G.M., Robinson, L.F., 2006. Interpretation of the $^{231}Pa/^{230}Th$ paleocirculation proxy: new water-column measurements from the southwest Indian Ocean. Earth Planet. Sci. Lett. 241, 493–504.

Toggweiler, J., 1999. Variation of atmospheric CO_2 by ventilation of the ocean's deepest water. Paleoceanography 14, 571–588.

Yu, J.M., Elderfield, H., 2007. Benthic foraminiferal B/Ca ratios reflect deep water carbonate saturation state. Earth Planet. Sci. Lett. 258, 73–86.

Yu, J., Elderfield, H., Piotrowski, A.M., 2008. Seawater carbonate ion-delta C-13 systematics and application to glacial–interglacial North Atlantic ocean circulation. Earth Planet. Sci. Lett. 271, 209–220.

Yu, J., Broecker, W.S., Elderfield, H., Jin, Z., McManus, J., Zhang, F., 2010a. Loss of carbon from the deep sea since the last glacial maximum. Science 330, 1084–1087.

Yu, J.M., Foster, G.L., Elderfield, H., Broecker, W.S., Clark, E., 2010b. An evaluation of benthic foraminiferal B/Ca and delta B-11 for deep ocean carbonate ion and pH reconstructions. Earth Planet. Sci. Lett. 293, 114–120.

Yu, J., Anderson, R.F., Jin, Z., Menviel, L., Zhang, F., Ryerson, F.J., Rohling, E.J., 2014. Deep South Atlantic carbonate chemistry and increased interocean deep water exchange during last deglaciation. Quat. Sci. Rev. 90, 80–89.

Yu, J., Menviel, L., Jin, Z.D., Thornalley, D.J.R., Barker, S., Marino, G., Rohling, E.J., Cai, Y., Zhang, F., Wang, X., Dai, Y., Chen, P., Broecker, W.S., 2016. Sequestration of carbon in the deep Atlantic during the last glaciation. Nat. Geosci. 9, 319–324.